Contrib Mineral Petrol (1984) 85:45–57

Contributions to Mineralogy and Petrology

Young Alpine dykes south of the Tauern Window (Austria): a K–Ar and Sr isotope study

Alexander Deutsch
Institut für Kristallographie und Petrographie, ETH-Zentrum, CH-8092 Zürich, Switzerland

Abstract. Fortyfive new K–Ar ages and Sr isotope data on amphiboles, biotites, clinopyroxenes and whole rock samples from subvolcanic dykes south of the Tauern Window establish, that alkalibasaltic dykes were intruded 30 m.y. ago and shoshonitic volcanism occured between 30 and 24 m.y. ago. Two calc-alkaline rocks of high-potassium composition yielded ages of 40 and 26 m.y. resp., a spread which may or may not be real. Calc-alkaline dykes with medium and low potassium contain excess argon and are hence undatable. Alkalibasaltic dykes have $^{87}Sr/^{86}Sr$ ratios of 0.7056–0.7070, shoshonitic rocks 0.7075–0.7133, potassium rich calc-alkaline dykes 0.7077–0.7100. $^{87}Sr/^{86}Sr$ of all other calc-alkaline rocks scatter between 0.7074 and 0.7150. Sr data indicate that dykes studied do not represent closed Sr systems, but that Sr characteristics result from selective strontium assimilation en route to surface. Primary Sr isotopic ratios of alkalibasaltic dykes point to an origin of these rocks in enriched sub-continental upper mantle. The source region of shoshonitic and high-potassium calc-alkaline rocks could have $^{87}Sr/^{86}Sr$ around 0.707, which is assigned to the input of a component rich in alkalies, LREE and LIL elements. Genetic relationships with other Tertiary magmatites of similar geotectonic position are explained in terms of plate tectonic models of the Eastern Alps.

Introduction and geological setting

Unfoliated dykes of varied chemical composition in the region south of the Tauern Window have been known since Teller (1889) and Canaval (1895). The alpine deformation and metamorphism are bracketed by these rocks. Moreover, they are a key to late alpine tectonic processes. Despite their importance, little geochemical work has previously been done, although some petrographic descriptions are available (Alker et al. 1952; Holzer and Scharbert 1958; Exner 1961; Heritsch 1971; Deutsch 1980).

The primary goal of this investigation was to establish age relationships between the different groups of dykes and to correlate them with the tonalitic bodies of Eocene to Oligocene age farther west, e.g. Rensenspitze (Borsi et al. 1978a), Rieserferner, Zinsnock, Altenberg (Borsi et al. 1978b), Adamello (Borsi et al. 1977; Cortecci et al. 1979; Hansmann and Oberli 1983; Kagami et al. 1983) and Bergell (Gulson and Krogh 1973; Deutsch and Steiger 1983). The new age determinations combined with Sr and trace element data are intended to constrain models of magma generation on the proposed subduction/collision zone (Hawkesworth et al. 1975; Frisch 1978, 1981; Dietrich 1976).

Figure 1 shows the location of the dykes investigated and outlines the geological situation. The Austroalpine unit consists of polymetamorphic crystalline basement rocks of unknown stratigraphic age ("Altkristallin") overlain by a Paleozoic metasedimentary sequence in the greenschist facies. Carboniferous to Albian sediments of the Drau chain rest unconformably upon the Altkristallin. To the south, the Gailtal crystalline unit as part of the Austroalpine unit is cut off by the Periadriatic line.

Isotopic ages of metamorphic minerals around the south-east corner of the Tauern Window cluster around 80 m.y. (Oxburgh et al. 1966; Cliff et al. 1971; Hawkesworth 1976). Young alpine mica ages around 20 m.y., however, noted in the Austroalpine basement in South Tyrol (Borsi et al. 1978b; Hammerschmidt 1981) and from localities inside the Tauern Window (Oxburgh et al. 1966) have not been reported from the area under study. Up to now, no comprehensive geological study of this region including all geochronological and petrological investigations has been published.

Petrographic and geochemical outlines

The dykes are two to ten meters thick. They crosscut the structures of the country rocks and do not display any cleavage; no other xenoliths than those of surrounding crystalline rocks were found. In a few samples resorbed quartz crystals and partly molten plagioclase xenocrysts are present.

According to major, trace and rare earth elements as well as mineral chemistry, the dykes can be grouped into:

* calc-alkaline rocks (CAB), concentrated in the Gailtal crystalline unit (Fig. 1), but also found in the northern Kreuzeck region
* a shoshonitic suite (SHOSH) in the southern Kreuzeck Mts. and in Albian sediments south of Lienz and
* an alkalibasaltic series (AB) which occur only in the Goldeck Mts. (Deutsch 1980).

Table 1 shows some petrographic characteristics of these groups; representative chemical analyses are listed in

Present adress: Inst. f. Mineralogie, Westf. Wilhelmsuniversität, Corrensstr. 24, D 4400 Münster, F.R.G.

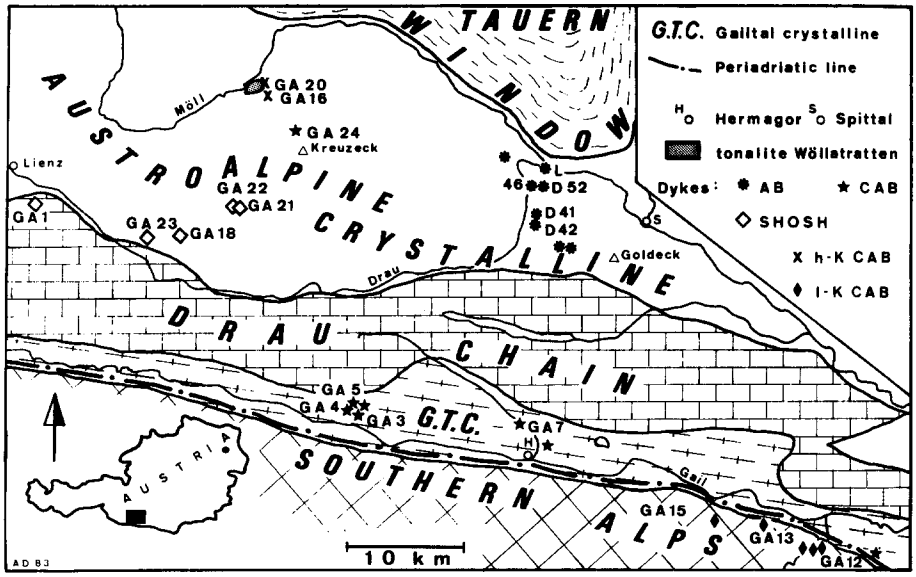

Fig. 1. Sketch map of the region between Lienz and Spittal/Drau (Austria) showing the sample locations and geological outlines. Dykes: AB = alkalibasaltic, SHOSH = shoshonitic, CAB = calc-alkaline, h-K CAB = high potassium calc-alkaline, l-K CAB = low potassium calc-alkaline

Table 1. Main petrographic features of the dykes investigated

Rock-type	Alkalibasaltic (AB)	Shoshonitic (SHOSH)	Calc-alkaline		
			High-potassium (h-K CAB)	Normal (CAB)	Low-potassium (l-K CAB)
main phases	kaersutite	titanian-biotite	ferroan-pargasitic hornblende	tschermakitic/ magnesio-hornblende	augite
	titanian pargasite/ hastingsite			biotite (rare)	edenitic/ magnesio-hornblende (rare)
	titanian-biotite	titanian-magnesian hastingsite			
	salite – Ti-augite	Ti-augite			
	alkalifeldspar	alkalifeldspar	plagioclase (An 71-35)	plagioclase (An 63-38)	plagioclase (An 68-17)
		plagioclase (An 71-35) mantled by K-feldspar	+ −quartz	+ −quartz	
phenocrysts	amphibole, biotite	amphibole, biotite (rare) clinopyroxene – cluster	amphibole (rare)	none	none
ocelli	frequent	rare	none	none	none

Table 2. Detailed discussion of the geochemical investigations will be the topic of another paper (Deutsch, in prep.). The distinction between alkaline and calc-alkaline series was made according to Irvine and Baragar (1971). Calc-alkaline rocks have been subdivided further using the K_2O vs SiO_2 discriminant of Peccerillo and Taylor (1976).

AB and SHOSH rocks form chemically homogenous groups with clearly defined trends in variation-diagrams, indicating a genesis from distinct parent magmas by fractional crystallization. Their overall geochemical features point to an intraplate tectonical setting.

The AB series ranges from *ne-* to *di-ol-hy* – normative rocks. They are rich in alkalies ($K_2O/Na_2O < 1$), incompatible elements and rare earth elements (REE). LREE are strongly fractionated (Ce_n/Yb_n 31 – 28); small negative Eu-anomalies (Eu/Eu* 0.88–0.76) can be recognised (Fig. 2a).

SHOSH dykes are characterized by a very high alkali content ($K_2O/Na_2O > 1$), titanium contents up to 2.5 wt.% (water-free) and by high concentrations of trace elements (especially Zr, Th, Ba) and fluids. LREE are even more fractionated than in the AB series ($Ce_n/Yb_n < 47$), patterns show steep HREE and no to insignificant negative Eu-anomalies with Eu/Eu* between 0.97 and 0.84 (Fig. 2b). More evolved rocks become *qz* + − *c* − normative and grade at northern Kreuzeck Mts. into the high-potassium calc-alkaline dykes (h-K CAB) GA-16 and GA-20, which have small negative Eu-anomalies (Eu/Eu* 0.8) and a Ce_n/Yb_n ratio around 10. In both groups (AB, SHOSH + h-K CAB) the lack of significant Eu-anomalies and the high Sr contents in the least evolved dykes preclude plagioclase as a significant residual phase in the source material; corresponding to pressure values over 10 kbar (Wyllie 1977).

Table 2. Analyses of selected samples from the different dyke groups. D 42 and D 52 from Deutsch (1980). Main and trace element analyses done by XRF techniques (Nisbet et al. 1979); REE, U, Th by neutron activation techniques (Bajo and Wyttenbach 1980); Sr and Rb by isotope dilution. n.d. = not determined

Group	AB		SHOSH			h-K CAB	CAB		l-K CAB	
Sample	D 42	D 52	GA-22	GA-18	GA-23	GA-16	GA-7	GA-5	GA-12C	
wt.%										
SiO_2	45.01	45.79	44.27	48.36	53.49	56.86	46.43	49.77	47.63	
TiO_2	2.21	1.85	1.84	1.56	1.33	0.64	1.47	1.74	1.10	
Al_2O_3	14.53	14.10	14.18	15.08	15.59	15.84	16.23	16.28	17.49	
Fe_2O_3	4.84	2.88	3.16	3.59	2.24	2.03	2.23	3.23	2.05	
FeO	5.53	6.97	5.75	5.15	4.75	3.85	7.20	6.90	6.40	
MnO	0.18	0.17	0.17	0.17	0.12	0.13	0.15	0.18	0.17	
MgO	9.14	8.90	6.53	6.96	6.53	5.39	7.70	6.91	8.11	
CaO	8.63	9.19	7.87	6.93	4.48	6.12	7.67	7.56	8.93	
Na_2O	2.75	2.61	2.42	2.62	2.99	3.30	2.55	2.64	3.16	
K_2O	2.34	2.15	2.81	3.92	3.41	2.51	0.85	1.15	0.11	
P_2O_5	0.82	0.58	0.88	0.80	0.35	0.23	0.33	0.50	0.18	
H_2O+	2.67	3.03	2.19	2.42	2.53	1.89	5.36	2.85	4.38	
CO_2	n.d.	n.d.	5.36	0.83	0.93	0.43	0.39	0.04	0.39	
Cr_2O_3	0.04	0.04	0.02	0.03	0.03	0.03	0.04	0.03	0.03	
NiO	0.03	0.02	0.02	0.02	0.02	0.00	0.02	0.01	0.01	
Total	98.72	98.28	97.47	98.44	98.79	99.25	98.62	99.79	100.14	
ppm										detection limits
Nb	54	26	36	34	19	3	0	14	0	3
Zr	271	209	388	372	261	149	190	297	91	4
Y	32	22	21	25	13	12	18	40	14	4
Sr	1,578	964	1,214	1,025	834	618	436	421	373	ID
U	43	8	15.2	12.6	11.9	6.4	<0.6	<0.6	<0.6	INAA
Rb	61.1	65.1	82.5	125	106	95.7	39.7	48	4.94	ID
Th	75	21	72.8	74.4	38.0	15.4	1.62	3.7	1.61	INAA
Pb	46	7	0	24	0	18	0	0	0	6
Ga	17	16	13	15	17	13	12	18	12	2
Zn	83	77	104	93	69	61	76	98	59	5
Cu	46	0	11	18	15	21	13	10	0	7
Ni	177	146	100	112	134	24	112	87	46	7
Co	47	42	25	27	19	12	43	41	44	6
Cr	279	325	211	223	273	219	289	220	248	10
V	276	253	243	254	229	181	161	93	168	3
Ba	1,453	946	1,408	1,536	1,042	653	216	223	55	2
Sc	28	34	23	27	26	27	25	26	33	0.4
S	510	8,572	1,426	99	582	416	1,006	0	805	16
La	157	59.6	207	198	74.6	37.7	23.2	24.5	9.76	
Ce	325	145	355	327	130	70.7	51.9	71.7	22.4	
Sm	15.3	7.54	19.1	16.5	8.38	5.71	6.58	7.27	3.48	
Eu	3.77	1.49	3.92	3.39	2.15	1.29	1.88	2.06	1.23	
Tb	1.74	<0.5	1.46	1.33	0.803	0.626	1.01	1.26	0.478	
Yb	2.7	1.3	1.93	2.45	1.85	1.77	3.02	3.3	1.92	
Lu	0.49	0.20	0.306	0.377	0.276	0.264	0.466	0.59	0.300	

Garnet, however, is expected in the residuum due to the enrichment of Tb over Yb. REE patterns and trace and major element trends point to a differentiation mainly governed by the fractionation of amphibole with minor amounts of clinopyroxene and feldspar. Clusters of amphiboles and clinopyroxenes are frequent in silica-poor rock types and are probably cumulates. Removal of apatite, a very common constituent of these dykes, reduced the total abundance of REE, a conclusion supported by the covariance of Ce and P_2O_5 and by the drastical lowering of phosphorus concentrations in SiO_2-rich rocks.

High-Al, low-K calc-alkaline rocks (l-K CAB) with TiO_2 around 1.0 wt.% have been found only in the basement of the Southern Alps, close to the Periadriatic line (in this region = Gailtal line). In variation diagrams they show smooth trends of most major elements as well as Cr, Co, Sc, V, Zn, and K/Rb. Alkalies; Ba, Sr, and Sr/Ba; and Ni scatter within wide ranges. Important features of l-K CAB dykes are the H_2O-poor primary mineralogy (augite – plagioclase), and REE patterns with slight enrichment of LREE relative to the flat HREE ($Ce_n/Yb_n \sim 3$) and a small positive Eu-anomaly ($Eu/Eu^* \sim 1.2$) (Fig. 2c).

Except for GA-24 from the central Kreuzeck Mts. basaltic to andesitic dykes with moderate potassium (CAB) are

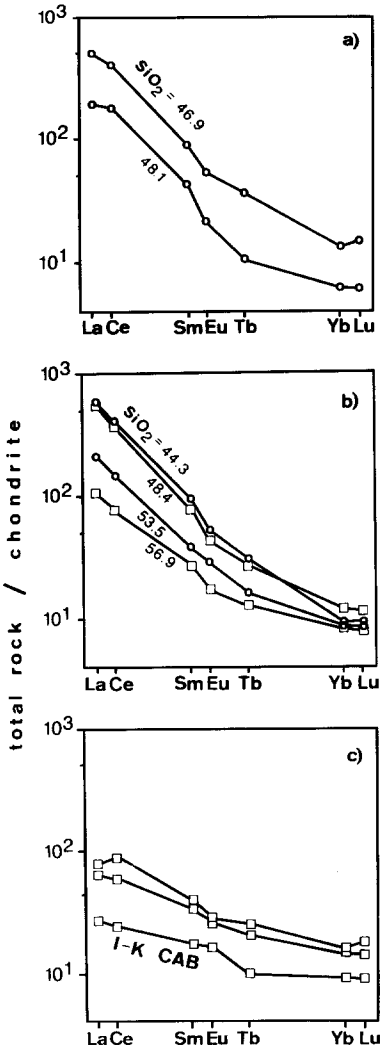

Fig. 2. REE contents of selected dykes (normalized to Leedy chondrite/1.2 of Masuda et al. 1973): (a) AB; SiO_2 recalculated on H_2O- and calcite-free basis (b) SHOSH and one h-K CAB; SiO_2 in wt.% is not recalculated on H_2O- and calcite-free basis because of the high and variable contents of primary fluids (c) l-K CAB and CAB dykes

concentrated north of the Gailtal line in a geotectonic position comparable to Rieserferner and Zinsnock plutons. It is remarkable that more acidic dyke rocks with calc-alkaline geochemical properties can be traced from the Rieserferner pluton to the Kreuzeck Mts. (Beck 1936). The CAB group ranges from *ol-hy-di* to *hy-qz-c* – normative rocks and displays significant variations in all measured elements (e.g. TiO_2 1.6–2.2 wt.% at $SiO_{2\ 50.5}$ [water-free]) which can not be related to any differentiation process. However, their REE patterns are relatively uniform with slightly fractionated LREE (Ce_n/Yb_n 5.6–4.4). La reaches 80 times the chondritic abundance; no or small negative Eu-anomalies with Eu/Eu* between 1. and 0.86 are visible (Fig. 2c).

Age relationships between the different groups can be established based on grade of hydrothermal alteration. AB, SHOSH, and h-K CAB dykes usually form fresh "lamprophyres", displaying some prehnite, pumpellyite, calcite, quartz, mixed layered minerals, epidote, and (in GA-1 only) analcime. The CAB and l-K CAB rocks were subjected to stronger alteration: among secondary phases actinolite in places pseudomorphically replaces primary amphiboles. These actinolite-bearing rocks were presumably intruded before the Austroalpine block had entirely cooled down.

Analytical techniques

Minerals were separated by standard techniques (i.e. heavy liquids, magnetic separator), handpicked and finally cleaned in ethanol with an ultrasonic cleaner. Each Rb–Sr whole rock sample originally weighed 10 to 20 kg and was carefully checked to avoid xenoliths and fissures.

Potassium was analyzed by isotope dilution. Pooled replicate analyses give an analytical error of $+-0.9\%$ at the 95% confidence level (95% CL).

Argon analyses were carried out on three different mass spectrometers.

1) Specimen indicated by an asterisk in Table 3 were measured unspiked on our all-metal mass spectrometer equipment which is normally used for extraterrestrial material. This instrument was described in detail by Signer et al. (1977). 12 runs of the standard muscovite P-207 with sample weights between 6.84 and 34.55 mg yielded an average radiogenic argon concentration of $2.859+-0.35\times10^{-5}$ cm^3 STP/g (95% CL). On some samples with low gas amounts, the uncertainty at radiogenic argon of 1.6×10^{-12} cm^3 STP ^{40}Ar caused by a "memory" of lunar samples (e.g. dust from bulk samples, mass spectrometer) may be important. This value is calculated assuming that measured argon extracted from pure Al foils with $^{40}Ar/^{36}Ar$-ratios between 240 and 90 is composed of an air and a lunar component and, further, by using replicate analyses. In isochron diagrams this uncertainty results in strongly correlated errors ($\varrho=0.9-0.99$) as shown in Figs. 3–6.

2) Therefore we repeated the argon determination of 4 samples for comparison at the Laboratorium für Geochronologie, Universität Heidelberg/FRG (inidicated by "H" in Table 3) using conventional isotope dilution techniques (Horn et al. 1972).

3) Nearly half of all argon analyses were performed with the peak height method (i.e. unspiked) in a new all metal rare-gas system consisting of an electron impact furnace, a newly developed purification line and a rebuilt MS MAT 240 with automated data acquisition. The mass spectrometer is operated in the static mode and has a 120 mm radius in 90° magnetic deflection. It is equipped with a Faraday collector and a multiplier on two exit slits and has a newly designed electron impact source with high linearity over a wide pressure range (Baur 1980). The mass spectrometer was calibrated with pure argon both volumetrically and by measuring pressure. This procedure, measurement technique and data reduction will be presented elsewhere (Baur, Deutsch, Signer in prep.). Eleven runs of the biotite standard LP-6 with sample weights between 6.61 and 31.86 mg resulted in mean value of $4.202+-0.027\times10^{-5}$ cm^3 STP/g for the radiogenic argon content.

Errors stated in Table 3 are 1 σ errors calculated by Gaussian error propagation. For this propagation the analytical error of K-determination and the error of the sample weight and the accuracy of the coefficients defining the regression lines for each individual Ar isotope measurement (40, 36) have been used.

Regression lines are calculated according to York (1969). Since the weighting factor is $1/\sigma^2$, this calculation scheme is not very suitable for presenting K–Ar data. Depending on the value of χ, quoted errors of isochrone ages and ($^{40}Ar/^{36}Ar$) intercepts are 2σ or $2\sigma\chi$. The data points in graphic presentations show 1 σ error ellipses unless the symbol size exceeds these errors.

For analytical techniques including data evaluation of Rb and Sr carried out with a VARIAN MAT CH 5 Tandem solid source mass spectrometer, we refer to Steiger et al. (1979). During the course of this work we obtained a mean normalized $^{87}Sr/^{86}Sr$ ratio of 0.71046 ± 0.00006 (95% CL) for NBS 987 (23 runs). Minerals were measured on a MAT 261 solid source mass spectrometer (labelled with an asterisk in Table 4). There our result for the NBS 987

Table 3. K-Ar dating results. *=noble gas equipment for extraterrestrial samples (ETH-Zürich). H=Laboratorium für Geochronologie der Universität Heidelberg/FRG. #=potassium determination by XRF. Errors=+−1σ. n.d.=not determined. Abbreviations as in Figs. 1, 3

Sample number	Material	Grain size	K	^{36}Ar	^{38}Ar	^{40}Ar	^{40}Ar	Weight	Calculated age	
		[Microns]	[ppm]	[in units 1×10^{-8} cm^3 STP/g]			[% rad]	[mg]	[m.y.]	
CAB dykes										
GA-5 *	amph	100–265	5,730	0.130	0.0240	704.7	95	26.5	277.0	+−2.8
GA-5A *	amph	41– 70	1,850	0.0852	0.01649	195.2	87	59.6	222	+−4
GA-7 *	cpx	41–100	1,019	0.134	0.022	425.3	91	34.3	779	+−10
GA-7 *	cpx leached	41– 70	954	0.028	0.0071	380.4	98	10.9	799	+−15
GA-24 *	WR	320–430	8,140	0.2156	0.03799	1,299.3	95	119.8	354	+−7
l-K CAB dykes										
GA-13B #	WR	320–430	7,640	0.1195	0.02143	702.4	95	109.8	212	+−4
h-K CAB dykes										
GA-16	amph	170–200	7,680	0.2882	0.0546	206.83	59	88.2	40.4	+−0.5
GA-16	amph	170–200	7,680	0.3426	0.0638	224.27	55	53.9	40.8	+−0.5
GA-20 *	amph	100–140	7,700	0.123	0.0227	114.9	68	23.7	26.1	+−0.7
SHOSH dykes										
GA-1 *	amph	210–265	10,840	0.143	0.0264	144.78	71	22.9	24.2	+−0.5
GA-1 *	amph	210–265	10,840	0.095	0.0170	130.79	79	26.1	24.3	+−0.5
GA-1 *	bi	58–100	62,800	0.186	0.0336	645.7	91	19.9	24.06	+−0.25
GA-1 H	bi	58–100	62,800	0.2584	n.d.	668.0	89	120.9	24.1	+−0.4
GA-1	bi	100–175	68,500	0.1596	0.02908	712.9	93	56.4	24.8	+−0.5
GA-18	amph	70–200	11,450	0.1456	0.02680	164.64	74	63.8	27.1	+−0.4
GA-18	amph	70–200	11,450	0.2014	0.03752	180.92	67	89.5	27.1	+−0.4
GA-18 *	bi	160–200	69,400	0.121	0.0242	753.0	95	22.8	26.40	+−0.31
GA-18	bi	160–200	69,400	0.7091	0.1329	921.6	77	14.7	26.21	+−0.31
GA-18	cpx	140–200	909	0.3438	0.0640	116.75	13	25.1	42.4	+−1.6
GA-18 #	WR	chips	32,500	0.4942	0.0917	666.7	78	141.8	40.7	+−0.8
GA-21 *	bi	220–265	75,900	0.085	0.0162	841.7	97	17.7	27.5	+−0.3
GA-21 *	bi	430–710	77,400	0.345	0.0642	935.8	89	13.0	27.5	+−0.4
GA-21 H	bi	430–710	77,400	0.2139	n.d.	877.0	93	133.3	26.9	+−0.4
GA-22 *	bi	180–265	70,000	0.194	0.0363	853.9	93	17.7	29.1	+−0.4
GA-22 *	bi	180–265	70,000	0.204	0.0387	863.3	93	7.7	29.3	+−0.4
GA-23 *	amph	140–200	11,750	0.208	0.0379	199.2	69	24.6	29.9	+−0.6
GA-23 *	bi	120–200	66,200	0.123	0.02331	755.5	95	32.2	27.8	+−0.3
GA-23	bi	120–200	66,200	0.2522	0.0469	770.5	90	25.8	26.89	+−0.28
AB dykes										
D 41	amph	100–190	11,070	0.1227	0.02271	163.82	78	56.1	29.41	+−0.30
D 41 *	amph	190–315	11,430	0.049	0.0097	147.0	90	19.2	29.6	+−0.6
D 42	amph	100–190	11,210	1.2160	0.2285	494.66	27	26.4	30.8	+−0.5
D 42	amph	190–315	11,110	0.2623	0.0489	206.85	63	43.0	29.7	+−0.4
D 46 *	amph	100–190	11,630	0.035	0.00654	148.3	93	44.8	30.3	+−0.4
D 46 *	amph	190–315	11,900	0.060	0.01195	158.09	89	31.9	30.1	+−0.5
D 46 H	amph	190–315	11,900	0.0816	n.d.	164.6	85	272.5	30.1	+−0.5
D 52 *	amph	65–100	9,730	0.060	0.0115	127.29	86	29.1	28.7	+−0.6
D 52	amph	65–100	9,730	0.3013	0.0566	202.86	56	32.2	29.9	+−0.4
D 52	amph	100–190	8,520	8.60	1.618	2,648	4	1.4	31.5	+−2.9
D 52 *	amph	190–315	9,860	0.048	0.00894	135.17	90	30.4	31.4	+−0.4
D 52 *	amph	190–315	9,860	0.038	0.0070	137.4	92	29.9	32.6	+−0.4
D 52 *	amph	190–315	9,860	0.0765	0.0147	139.6	84	49.4	30.3	+−0.5
D 52	amph	190–315	9,860	0.1602	0.02966	163.80	71	93.6	30.2	+−0.6
D 52 H	amph	190–315	9,860	0.0805	n.d.	139.0	83	217.2	29.8	+−0.5
D 52 #	WR	chips	21,500	0.2944	0.05397	423.1	79	185.6	39.8	+−0.7

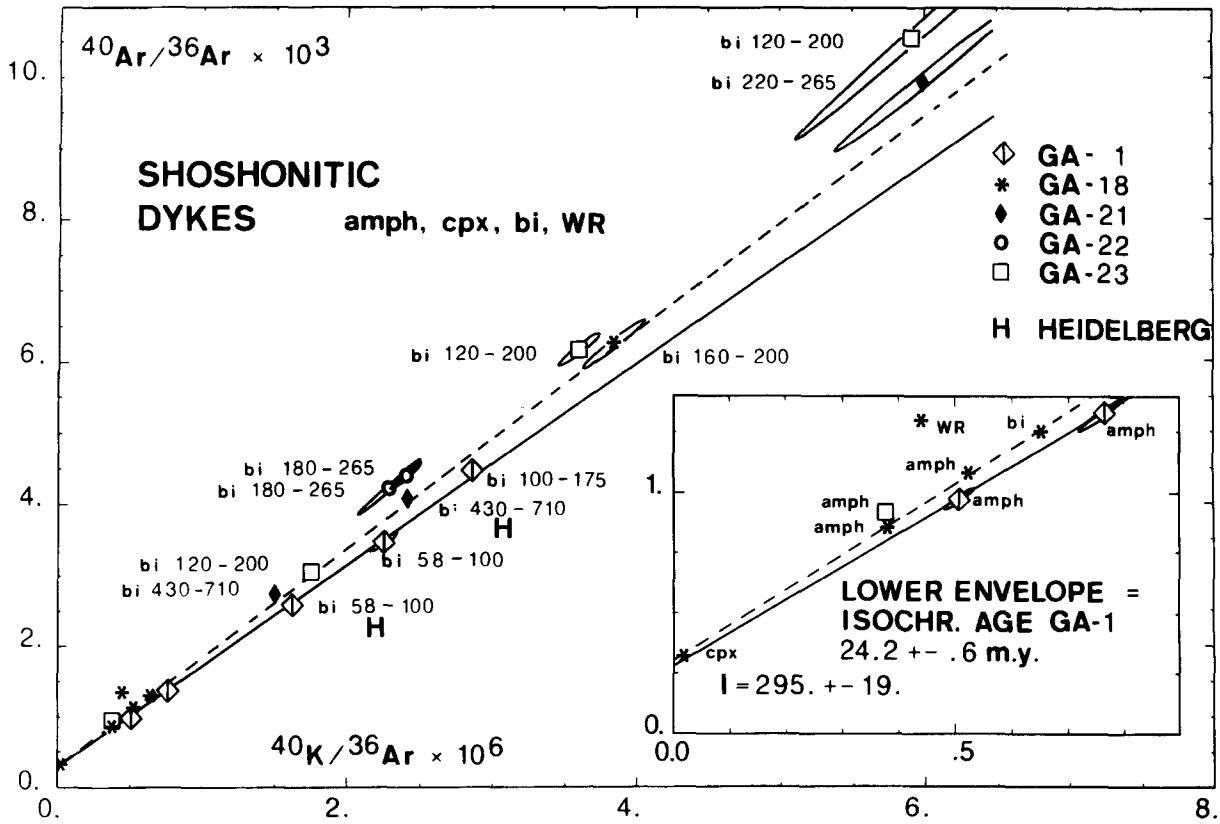

Fig. 3. $^{40}Ar/^{36}Ar$ versus $^{40}K/^{36}Ar$ diagram concerning all measured minerals from SHOSH dykes. The isochron for GA-1 forms the lower envelope. The dashed line represents a pseudoisochrone (age: 26.0+ −0.8 m.y., I=313. + −15.0), calculated by using all data from this rock suite. Amph = amphibole, cpx = clinopyroxene, bi = biotite, WR = whole rock. Numbers stand for grain size in μm

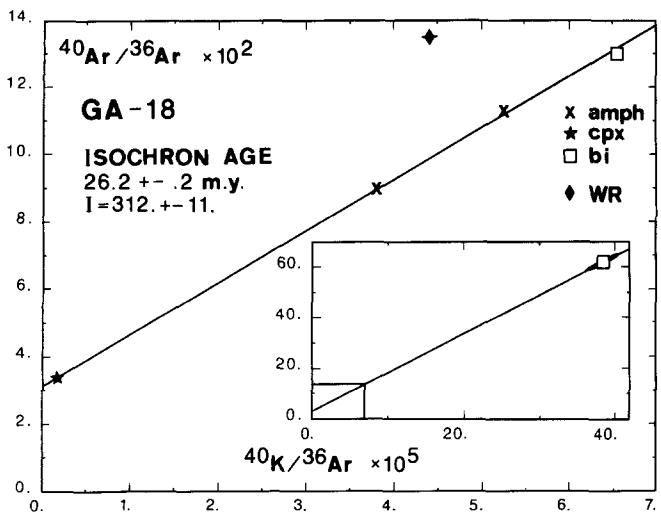

Fig. 4. $^{40}Ar/^{36}Ar$ versus $^{40}K/^{36}Ar$ diagram for sample GA-18. Note that the whole rock plots far above the isochron which gives the intrusion age of this SHOSH dyke. Abbreviations as in Fig. 3

standard is 0.710238 [12]. Due to this difference all normalized $^{87}Sr/^{86}Sr$ ratios were adjusted to the NBS-value of 0.71014. The maximum error for $^{87}Rb/^{86}Sr$ is + −2%, for $^{87}Sr/^{86}Sr$ we give the individual standard error at 95% CL.

Decay constants and atomic ratios as recommended by the IUGS Subcommission on Geochronology (Steiger and Jäger 1977) have been used.

Results of K−Ar dating (Table 3)

CAB and l-K CAB group. Because of excess argon no geologically useful results were obtained.

Mineral concentrates (checked by microprobe for alteration products in grain mounts) as well as whole rock samples revealed various amounts of excess argon. Removing the outer rim of the clinopyroxene GA-7 by acid etching (Etique et al. 1978) shows that this excess radiogenic argon is distributed throughout the grains. Assuming a Tertiary age, the excess $^{40}Ar^*$ for the augite is in the order of 4.0×10^{-6} cm³ STP/g. These dykes underwent a marked alteration and radiogenic argon from Variscan metamorphosed country rocks dissolved in water probably pervaded these rocks during a hydrothermal stage. From our investigation it is evident that this argon is not only concentrated in secondary minerals.

H-K CAB dykes from the Kreuzeck area. Amphiboles from sample GA-16 yield a model age of 40.6 m.y., and sample GA-20 with very similar geochemical features shows an amphibole model age of 26.1 my. These dykes are in close genetic relationship with the Wöllatratten tonalite stock (Exner 1961), GA-20 crosscuts this magmatic body. In 1971 Cliff et al. published K−Ar data for biotite from the tonalite and found ages varying between 31. and 44. m.y. It is a question whether this spread in mineral ages is indicative for excess ^{40}Ar or simply displays a multi-stage emplacement as found in the Adamello massif (Borsi et al. 1977; Cortecci et al. 1979).

SHOSH group. The K−Ar results dykes yield a com-

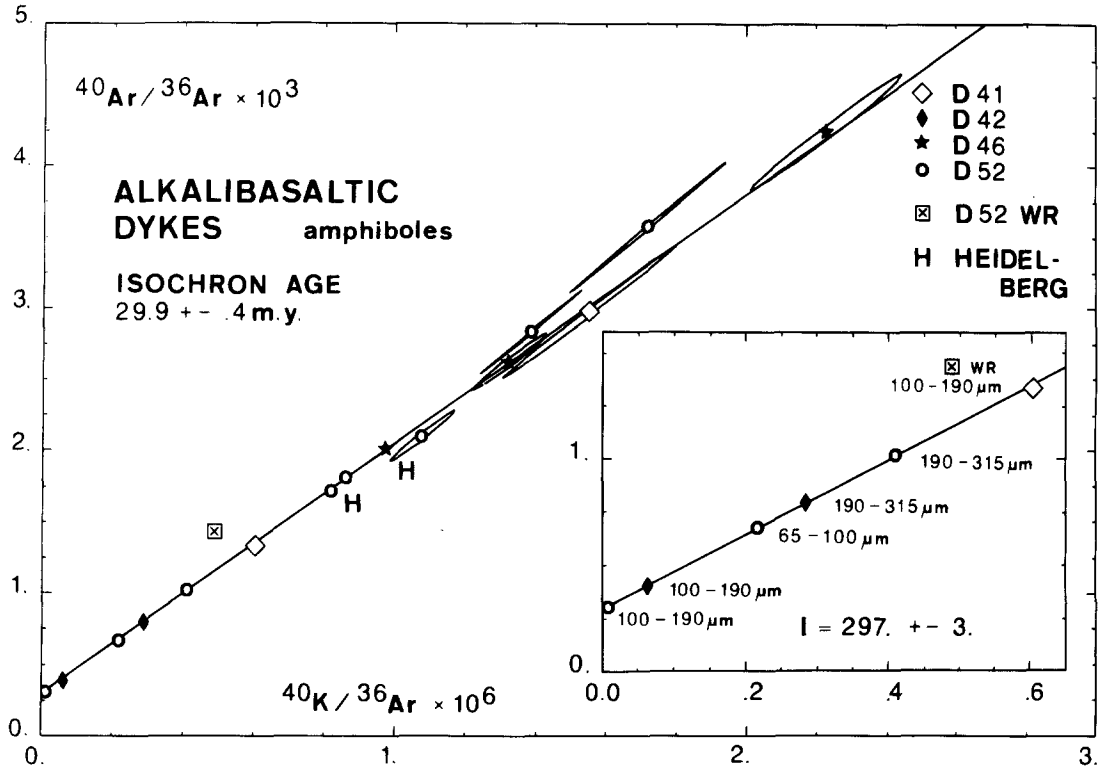

Fig. 5. $^{40}Ar/^{36}Ar$ versus $^{40}K/^{36}Ar$ diagram showing all data points from AB dykes. The isochron corresponds to the intrusion age of the AB suite

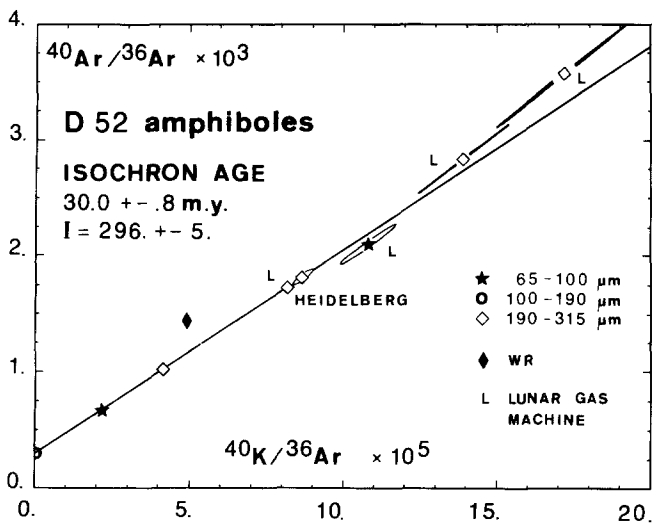

Fig. 6. $^{40}Ar/^{36}Ar$ versus $^{40}K/^{36}Ar$ diagram for AB sample D 52. Matrix amphiboles and phenocrysts fit an isochron defining the intrusion age whereas the whole rock displays some excess 40 Ar*

plex picture. Model ages of minerals range between 24.1 and 42.4 m.y.

In the entire region investigated the dyke SE of Lienz (GA-1) is the youngest example of volcanic activity. It has a well established isochron age of 24.2 m.y., connected with a $(^{40}Ar/^{36}Ar)^0$ ratio of 295.0 (Fig. 3).

An upper limit for the age of SHOSH dykes is indicated by the model ages of amphibole GA-23 (29.9 m.y.) and biotite GA-22 (29.2 m.y.), and is consistent with Rb–Sr data (p 8, Fig. 8a).

From regression line calculation done by using all 18 data points obtained for SHOSH rocks (Fig. 3), it is clear that the different dykes do not pertain to one single magmatic event, but were rather generated during a 5 m.y. span of time in the upper Oligocene.

In Fig. 4 the $^{40}Ar/^{36}Ar$ versus $^{40}K/^{36}Ar$ plot for sample GA-18 is given. Clearly, the whole rock contains excess ^{40}Ar and the intercept of 312.4 + −22.0 led to the conclusion that measured phases of GA-18 may have excess ^{40}Ar, too. Inferred from model ages this $^{40}Ar^*$ becomes critical only for the augite. Amphibole and biotite are unlikely to have gained excess ^{40}Ar in detectable amounts. Their model ages nearly agree within the gives 1 σ errors and correspond well to the isochron age of 26.2 + −0.2 m.y.

Although all dated SHOSH dykes show alteration products the K–Ar system of amphiboles and biotites seems to have remained closed at temperatures above 220° C and low pressure. These conditions can be inferred from experimental data for pumpellyite formation (Schiffman and Liou 1980) and from observations in deep drill holes (Sigvaldason 1962).

AB group. As no other phases than amphiboles could be separated, grain size suites of amphiboles have been investigated. The mineral model ages agree well with the isochron age in Fig. 5. This is strong evidence of all dykes of this group having been formed in one single event at 30.0 m.y. All $(^{40}Ar/^{36}Ar)^0$ ratios scatter around 295.5 (Figs. 5, 6) and no measurable difference between phenocrysts and groundmass amphiboles could be detected (Fig. 6). Both facts indicate that later hydrothermal processes did not significantly affect the K–Ar system of these magmatic amphiboles. The only whole rock sample measured (D 52), however, obviously contains excess radiogenic ^{40}Ar, probably trapped in alteration products.

Table 4. Rb–Sr analytical results. The maximum error for $^{87}Rb/^{86}Sr$ is +−2%. Errors (standard error at 95% CL) refer to the last digits of $(^{87}Sr/^{86}Sr)_{norm}$. $(^{87}Sr/^{86}Sr)_{norm}$ are adjusted to NBS=0.71014. SiO_2 and K_2O in wt.% recalculated on a H_2O- and calcite-free basis. However, one should note that rocks of the SHOSH suite contain primary fluids in considerable amounts. Abbreviations as in Figs. 1, 3

		SiO_2	K_2O	Rb ppm	Sr ppm	$^{87}Rb/^{86}Sr$	$(^{87}Sr/^{86}Sr)_{norm}$
CAB dykes							
GA-3	WR	55.2	2.04	102	305	0.9727	0.71497 (29)
GA-4	WR	56.0	1.65	54.0	406	0.3851	0.70799 (22)
GA-5	WR	51.4	1.19	48.0	421	0.3297	0.70793 (17)
GA-7	WR	50.3	0.92	39.7	436	0.2636	0.70895 (19)
GA-24	WR	50.7	1.01	40.2	363	0.3206	0.70737 (29)
1-K CAB dykes							
GA-12B	WR	49.0	0.13	4.84	441	0.03180	0.71298 (19)
GA-12C	WR	50.2	0.12	4.94	373	0.03835	0.71228 (37)
GA-13B	WR	54.6	0.97	33.2	267	0.3598	0.70817 (14)
GA-15B	WR	54.6	0.83	28.7	502	0.1653	0.70928 (20)
h-K CAB dykes							
GA-16	WR	59.0	2.60	95.7	618	0.4483	0.70989 (19)
	amph			15.8	245	0.1861	0.70772 (33) *
GA-20	WR	58.9	2.53	74.2	690	0.3114	0.70904 (22)
	amph			5.89	246	0.06936	0.70806 (10) *
SHOSH dykes							
GA-1	WR	46.4	3.75	69.4	1,139	0.1764	0.70806 (18)
GA-18	WR	51.4	4.16	125	1,025	0.3533	0.70905 (14)
	amph			11.2	906	0.03587	0.70800 (6) *
	bi			357.0	201	5.129	0.71012 (13) *
	cpx			3.08	150	0.05944	0.70814 (33) *
GA-21	WR	53.3	4.26	117	1,199	0.2816	0.70794 (24)
GA-22	WR	53.3	3.38	82.5	1,214	0.1968	0.70897 (10) *
GA-23	WR	56.8	3.62	106	834	0.3669	0.71328 (18)
	amph			10.0	523	0.05533	0.70746 (15) *
	bi			362	128	8.184	0.71112 (11) *
AB dykes							
L	WR	46.6	1.93	51.6	1,749	0.08527	0.70580 (22)
D 41	WR	47.7	2.63	67.5	1,083	0.1804	0.70698 (13)
D 42	WR	46.9	2.44	61.1	1,578	0.1120	0.70620 (23)
	amph			12.5	1,383	0.02617	0.70560 (10) *
D 46	WR	48.3	2.97	83.3	1,162	0.2074	0.70701 (17)
D 52	WR	48.1	2.26	65.1	964	0.1956	0.70700 (20)
	amph			7.07	723	0.02828	0.70619 (14) *

Rb–Sr results (Table 4)

Since an open K–Ar system in several different whole rock samples could be demonstrated, the main question was whether present day Sr isotope ratios of whole rocks would give any evidence about the source region of the magmas or simply would reflect contamination with Sr from Variscan metamorphosed country rocks induced by postmagmatic fluid circulation. For this, and for comparison with K–Ar dating results, a few highly purified amphiboles, two biotites and one clinopyroxene were analysed, too. Because of the very low Rb/Sr ratios of whole rocks and minerals (except for biotite) it is not necessary to correct measured Sr isotope ratios for accretion of ^{87}Sr by radioactive decay during the past 30 million years.

AB dykes have unusually high Sr contents up to 1,750 ppm. They show a tendency of increasing Rb/Sr and of increasing $^{87}Sr/^{86}Sr$ from 0.7058 to 0.7070 with differentiation, accompanied by a decrease in Sr concentration (Fig. 7a, b). $^{87}Sr/^{86}Sr$ ratios in two amphiboles are clearly lower than those of corresponding whole rocks.

SHOSH dykes exhibit more extended $^{87}Sr/^{86}Sr$ from 0.7079 to 0.7133. GA-23 with the highest Sr isotope ratio displays low Sr abundance (Fig. 7a) and has a high differentiation index (D.I.) (Fig. 7b). Thus this rock is more susceptible to contamination by highly radiogenic Sr in low abundance as expected from crustal rocks. A Sr isochron diagram (Fig. 8a) shows that this whole rock plots far above the line, connecting amphibole and biotite. The age corresponding to the slope (31.7+−1.7 m.y.), however, agrees well with K–Ar mineral ages of GA-23 (Table 3). Just the same is found on GA-18 (isochron age 29.3+−4.1 m.y., Fig. 8b) and both intercepts of 0.7074 (3) and 0.7080 (1) resp. coincide with the lowest present day ratios of analysed SHOSH whole rock samples. The low Rb/Sr ratios of analyzed biotites are due to apatite inclusions visible under microscope.

H-K CAB dykes with $^{87}Sr/^{86}Sr$ of 0.7099 and 0.7090

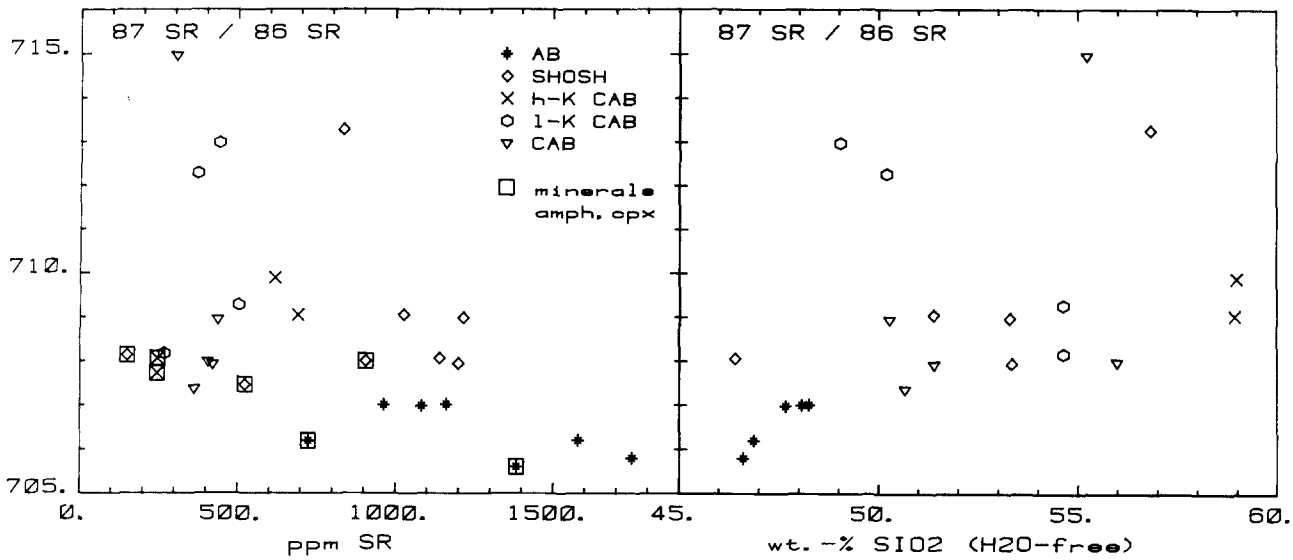

Fig. 7. **a** $^{87}Sr/^{86}Sr$ and Sr content variation of analyzed whole rocks and minerals. **b** $^{87}Sr/^{86}Sr$ versus wt.% SiO_2 (recalculated on H_2O- and calcite-free basis)

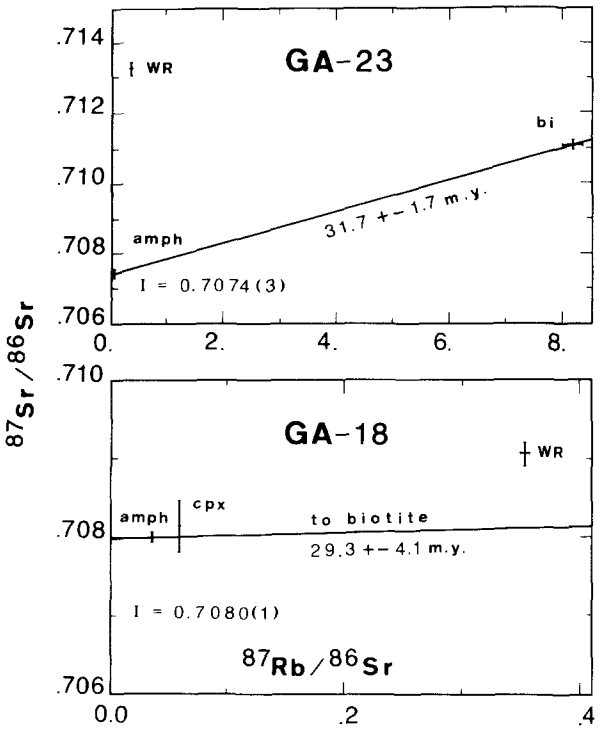

Fig. 8a, b. Sr – isochron diagrams for SHOSH dykes GA-23 (**a**) and GA-18 (**b**). Both whole rocks gained radiogenic Sr in a late stage of evolution. The mineral-isochrons correspond to the intrusion ages. Abbreviations as in Fig. 3

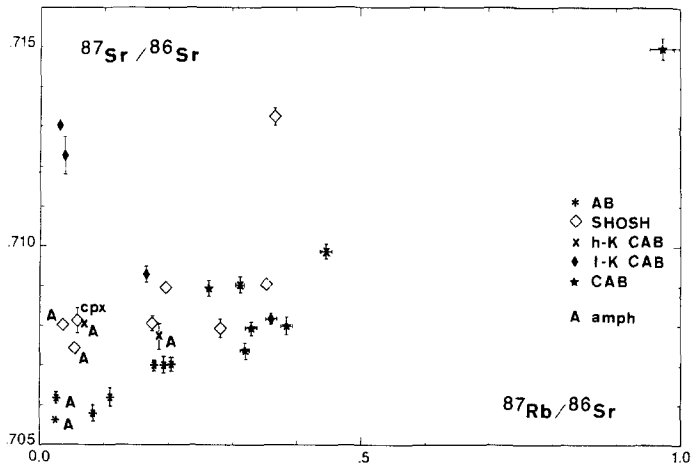

Fig. 9. Sr evolution diagram for all measured samples. Abbreviations as in Fig. 3

in whole rock samples also seem to have gained Sr of more radiogenic composition since their amphiboles show $^{87}Sr/^{86}Sr$ ratios of 0.7077 and 0.7081, respectively, as do amphiboles and one clinopyroxene from the SHOSH suite (0.7075 – 0.7081).

$^{87}Sr/^{86}Sr$ in l-K CAB whole rock samples decreases drastically from 0.7130 to 0.7082 with increasing SiO_2 (Fig. 7b) at nearly the same Sr content, whereas Rb/Sr shows the opposite tendency (Fig. 9).

$^{87}Sr/^{86}Sr$ in normal CAB dykes displays no dependance on Sr or SiO_2 concentrations (Fig. 7a, b) and varies from 0.7074 to 0.7090, except for GA-3. This rock displaying unusually high Rb/Sr of 0.334 combined with $^{87}Sr/^{86}Sr$ of 0.715 could have been contaminated in a postmagmatic stage since sample GA-4 on the same SiO_2-level yields much lower ratios of 0.133 (Rb/Sr) and 0.708 ($^{87}Sr/^{86}Sr$).

Discussion of Rb/Sr results

Compared with whole rocks, phenocrysts analysed from the AB and SHOSH + h-K CAB group have distinctly lower $^{87}Sr/^{86}Sr$. This points to contamination of the magma, after the phenocrysts grew, and at a higher crustal level. Bulk assimilation of larger quantities of crustal rocks can hardly account for this Sr with a more radiogenic component because major and trace elements form relatively smooth trends with D.I. in these dyke groups.

A possible mechanism for bringing Sr with a high isotope ratio into magma is selective assimilation or leach-

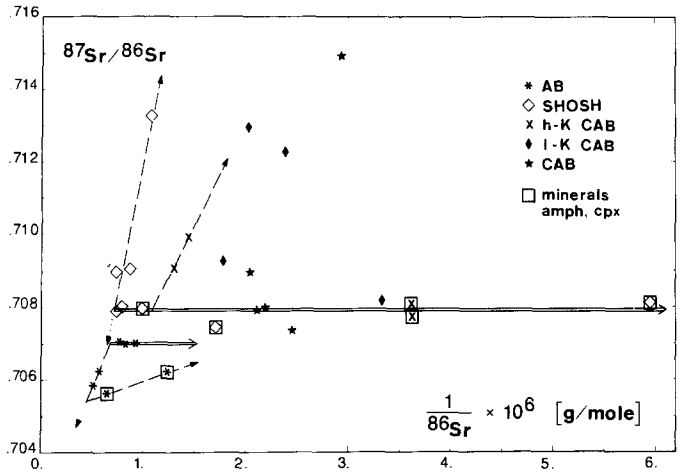

Fig. 10. $^{87}Sr/^{86}Sr$ versus $^{1/86}Sr$ plot. Dashed arrows show the change in $^{87}Sr/^{86}Sr$ by selective Sr contamination during a late stage of fractional crystallization. SHOSH whole rocks plot with increasing SiO_2 content in the direction of higher Sr isotope ratios; so do AB whole rocks with low silica. Full lines give the fractionation trend. Minerals are arranged according to their decreasing mg-value, AB whole rocks according to their increasing D.I. CAB and l-K CAB whole rocks plot independent of D.I. Abbreviations as in Figs. 1, 3.

ing while the magma is ascending through continental crust. Briqueu and Lancelot (1979) present a model involving processes of fractional crystallization combined with assimilation of crustal Sr transported by a fluid phase to explain anomalous $^{87}Sr/^{86}Sr$ ratios in calc-alkaline rocks. In a $^{87}Sr/^{86}Sr$ versus $^{1/86}Sr$ diagram, a line with a negative slope defines a mixing line between magma and a contaminating component whose maximum possible Sr isotopic ratio is given by the intercept on the ordinate. As differentation does not change the Sr isotopic composition, fractional crystallization in this graph is represented by a horizontal line. Vectors in between are a result of a combination of both, selective assimilation and fractional crystallization.

Using this type of graphic presentation (Fig. 10) variations of $^{87}Sr/^{86}Sr$ within AB, SHOSH + h − K CAB series can be explained satisfactorily.

Less evolved AB rocks (L, D 42) define a line indicative of selective contamination during early stages of fractionation, as do amphiboles, though with a lower degree of contamination. AB dykes with higher D.I. define a trend parallel to the x-axis showing that Sr contamination at this stage is negligible. The Sr isotopic ratio of initial magma cannot be deduced accurately from the diagram, but $^{87}Sr/^{86}Sr$ should be around 0.705. The high Sr content should make the AB magma fairly immune to having its Sr isotopic ratio raised by low Sr high $^{87}Sr/^{86}Sr$ crustal rocks. Therefore the ratio of 0.705 is attributed to the upper mantle which is seen as the source region of these rocks. For sub-continental mantle $^{87}Sr/^{86}Sr$ values in this range are reported by Manzies and Murthy (1980).

SHOSH whole rock samples define a steep line and the line connecting h-K CAB rocks GA-16 and GA-20 has a similar steep slope. Both are indicative of selective Sr contamination en route to the surface. Amphiboles and one clinopyroxene from both groups lie on a horizontal line, arranged to their decreasing mg-values, and were formed before the inferred high-level contamination took place. Remaining liquid, however, assimilated Sr rich in a radiogenic component until the final stage of differentiation. The difference between $^{87}Sr/^{86}Sr$ in minerals and $^{87}Sr/^{86}Sr$ in whole rock samples gives evidence for rapid cooling which prevented an isotopic homogenisation between phenocrysts and liquid. $^{87}Sr/^{86}Sr$ around 0.707 is regarded as a primary feature of the parental magma of SHOSH and h-K CAB dykes. In addition this magma is low in silica (GA-1), and has high abundances of alkalies, Th, Sr, Ba, and LREE. If in this case the upper mantle is also the source region, as expected, the introduction of the above stated elements has to be considered. The high content of $CO_2 + H_2O$ in the least evolved dykes (e.g. GA-22 with 5.36% CO_2) may hint at a transport into the mantle by fluids.

Some of the scatter obtained in $^{87}Sr/^{86}Sr$ in the l-K as well as in the CAB group may be due to hydrothermal alteration. However, Sr isotopic ratios from 0.7074 to 0.709 combined with relatively low Sr contents and low Rb/Sr ratios cannot be explained as a result of large scale interactions with Variscan metamorphosed gneisses and mica-schists. Indications for a crustal origin of this rock series are seen in the wide variations of trace elements (Ni, Ba, Rb) and in the variable corundum contents in the CIPW-norm. Our data are not sufficient to establish the presence of a mantle component in l-K CAB and CAB dykes although a contribution of material with low radiogenic Sr seems very likely.

Comparison with other Tertiary magmatites along the Periadriatic line (Fig. 11)

Among several post-Paleocene intrusions and dykes in the region south of the Tauern Window (cf. Exner 1976), the geochemistry of some tonalitic to granodioritic plutons is well-studied. The plutons display many features identical with the dykes under consideration: The geotectonic position, almost the same emplacement ages, homogeneous distribution of major elements and comparable Sr characteristics.

Tonalites from Rensenspitz massif have $^{87}Sr/^{86}Sr$ as low as 0.707, although the initial value of a whole rock isochron defined by granite samples is 0.7097 (Borsi et al. 1978a).

Sr isotopic ratio obtained for the small Altenberg pluton is 0.711. Its intrusion age must be somewhat greater than the weak metamorphic overprint at 23.0 m.y. which is recorded by biotite rejuvenation (Borsi et al. 1978b).

Two samples from the Zinsnock massif gave 0.708 (Borsi et al. 1978b), a biotite – whole rock isochron yields an age of 29.5 + − 1.1 m.y.

In the Rieserferner complex initial Sr isotope ratios of whole rock and mineral – whole rock isochrons range between 0.709 and 0.7207 and rocks displaying lower Sr abundances have the highest $^{87}Sr/^{86}Sr$ (Borsi et al. 1978b).

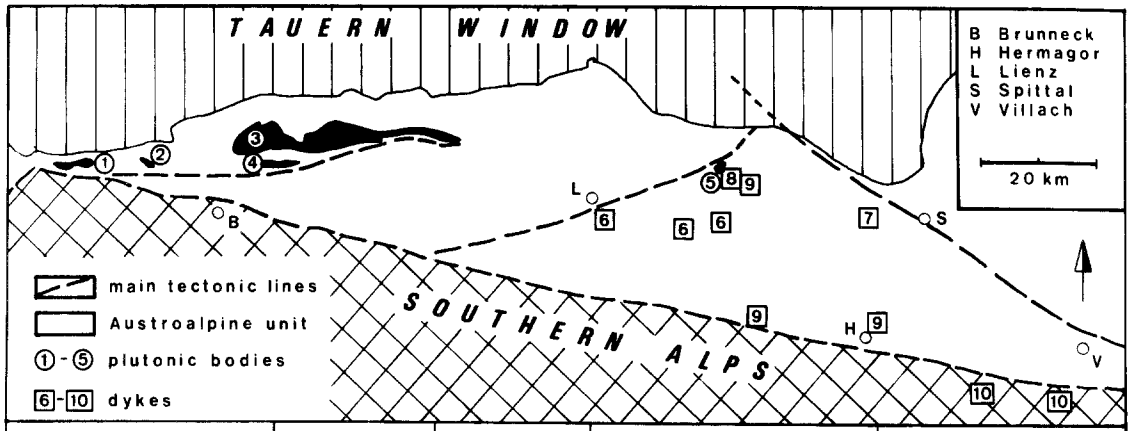

		$(^{87}Sr/^{86}Sr)_0$	intrusion age m.y.	method		
①	Rensenspitze	.7070-.7117	29.8±2.8	Rb/Sr	Mu-Wr	BORSI et al. (1978a)
②	Altenberg	.7111	>23.	Rb/Sr	$Bi_{metam.}$	BORSI et al. (1978b)
③	Rieserferner	.7089-.7207	30.±3.	Rb/Sr	Wr	
④	Zinsnock	.7079	29.5±1.1	Rb/Sr	Bi-Wr	
⑤	Wöllatratten		31.-44.	K/Ar	Bi	CLIFF et al. (1971)
6	SHOSH	.7075-.7133	24.2-31.7	K/Ar, Rb/Sr		
7	AB	.7056-.7070	29.9±.4	K/Ar		this work
8	h-K CAB	.7077-.7099	26.1-40.6	K/Ar		
9	CAB	.7074-.7090	?			
10	l-K CAB	.7082-.7130	?			

Fig. 11. Synoptical map of the area S of the Tauern Window with the location of Tertiary magmatites. Numerous dykes of various composition – here not mentioned – are located between the Rensenspitz massif and Spittal/Drau. Abbreviations as in Fig. 1

Surprisingly enough REE patterns from h-K CAB rocks (Fig. 2b) with similar Sr isotope ratios coincide with those observed in tonalites from the Rieserferner plutonic complex (Bellieni et al. 1981).

Borsi et al. (1978b) explained magma generation of these young alpine plutonites by anatexis and concluded that the wide spread of $^{87}Sr/^{86}Sr$ had been caused by different degrees of partial melting of crustal material. v. Gyzycki and Schmidt (1978) proposed that the formation of these melts by anatexis might have been supported considerably by strain-heat caused by intraplate deformation during the collision of the European and the African continent. Bellieni (1980) assumed that tonalites and granodiorites had been generated by high-pressure crustal melting followed by low-pressure fractionation processes. Based on REE and trace element data Bellieni et al. (1981) suggested that the Rieserferner suite represents a high-potassium "Andean"-type series resulting from crystal/liquid fractionation processes from one parent magma, possibly of dioritic composition. The scatter of the $^{87}Sr/^{86}Sr$ ratios might be a product of slight contamination with highly radiogenic crustal material, typical for calc-alkaline series emplaced on an active continental margin characterized by high crustal thickness (Thorpe and Francis 1979). Dupuy et al. (1982) postulated a similar genesis for the Adamello complex. According to their model the different rock types (gabbros – quartzdiorites) were produced from one parental magma with a composition similar to that of high-alumina basalts. The wide range of Sr isotope ratios observed could be explained satisfactorily by assimilation combined with fractionation processes. Recently Kagami et al. (1983) could confirm with a Nd – Sr study a mantle source for the ultramafic cumulates and for the gabbros in the Adamello. In contrast the slightly negative ε_{Nd} of -6.0 to -4.8 and higher $^{87}Sr/^{86}Sr$ of 0.7067 to 0.7071 of the intermediate intrusives point to the presence of an crustal component in this calc-alkaline series. This conclusion is supported by the occurence of zircons containing an inherited old Pb component of Precambrian origin (Hansmann and Oberli 1983).

In the prevailing plate tectonic models considering the evolution of the Eastern Alps (Hawkesworth et al. 1975; Dietrich 1976; Frisch 1978, 1981), the Austroalpine block as part of a proposed Adriatic plate overrides South Penninic units in the middle Cretacious. Except for one andesitic dyke in SW Tyrol with a questionable K–Ar whole rock age of $89.0+-7.0$ m.y. (Gatto et al. 1976) and alkalibasaltic dykes of perhaps Cretaceous age in the Northern Calcareous Alps (Trommsdorff 1962), there is no evidence for a Cretaceous magmatism.

According to Dal Piaz (1974) the widespread Tertiary magmatism should be linked to the Cretaceous subduction as a delayed affect. However, it seems more reasonable to connect the Tertiary magmatic rocks with the consumption of the North Prenninic ocean, which terminates in the late Ecocene with the second continent – continent collision (Frisch 1978). Timing and geochemical features (e.g. high-titanium shoshonites, intraplate alkalibasalts) clearly relate this magmatism to the post-collisional stage; but liquids initiating a partial melting of mantle material may still have been derived from the subducted Penninic oceanic crust. The different magma types – epiplutonic tonalites, hypabyssal shoshonitic associations, and alkalibasaltic rocks – may

be related to the degree and depth of partial melting and to the degree of hydratisation of the mantle peridotite (Takahashi et al. 1981). The uprise of the magmas coincides with an extensional regime in the Alps within the Oligocene (Laubscher 1983). In the region of proposed magma generation we have to consider an anormalous thick crust 30 m.y. ago caused by a pile consisting of the Austroalpine thrust sheet and various Penninic units. Inside the Tauern Window given maximum temperatures for the 40 m.y. old amphibolite metamorphism are 630° C + −20° C (Hoernes and Friedrichsen 1974) and the estimation of pressure for the deepest Penninic unit that is exposed today yields about 6 kbar (Cliff et al. 1971). Oxburgh and Turcotte (1974) showed with an analytical thermal model that the temperatures required for this metamorphism can not be attained without a contribution of heat from the upper mantle. England (1978) rejected this model and argued that there is little evidence for a large amount of igneous activity along the axis of the Austrian and Swiss Alps. However, there are numerous intrusions of similar age in this region (cf. Exner 1976).

The dykes investigated in the present study are part of this Oligocene-age event. Sr isotopic ratios of 0.705 for the primary AB melt point to an already enriched subcontinental mantle. For parental magma of SHOSH + h-K CAB dykes we have to consider the introduction of selected elements from the subducted material into the mantle by fluids (cf. Hawkesworth et al. 1979; Pearce 1982). Although the contribution of the downgoing slab can not be evaluated accurately, at least some Sr of more radiogenic composition and LREE, potassium and other LIL elements could have been introduced. The mobilization of these elements is caused by dehydration of the subducted slab and escape of the released fluids.

Conclusions

Mafic dykes found south of the Tauern Window can be classified into alkalibasaltic rocks (AB), into a shoshonitic suite (SHOSH) which grade into more andesitic high-potassium rocks (h-K CAB), and into calc-alkaline dykes (CAB) with low-potassium members (l-K CAB).

K − Ar data reported from minerals of these different dyke groups give clear age relationships:

1) AB rocks belong to a single magmatic event taking place 30 m.y. ago

2) rocks of the SHOSH group intruded between 30 m.y. and 24 my. ago

3) amphiboles from two h-K CAB dykes yielded ages of 40 m.y. and 26 m.y., respectively, but significance is not known

4) because of their stronger alteration CAB and l-K CAB dykes are believed to be somewhat older than 30 m.y.; their mineral ages indicated various amounts of excess argon 40.

The Rb/Sr systems show complexity: early crystallized mafic phases such as amphibole and clinopyroxene provide some information about Sr characteristics of the primary magmas whereas remaining liquids assimilated Sr enriched in a radiogenic component during their ascent. In the case of AB, SHOSH + h-K CAB rocks higher Sr isotopic ratios in rocks with higher D.I. can be explained by a combined process of fractionation and selective Sr contamination. From our data we can estimate initial $^{87}Sr/^{86}Sr$ ratios around 0.705 for AB melt. This value is compatible with a magma generation in the enriched sub-continental mantle as required to fit the geochemical and mineralogical data of this series. Sr isotopic ratio of 0.707 for the parental melt of the SHOSH + h-K CAB suite is connected with strong enrichment in LREE, K and LIL elements, which could be caused by fluid transport into the mantle prior to fractionation. $^{87}Sr/^{86}Sr$ together with wide variations in some trace elements, as found in CAB and l-K CAB dykes, indicate a major contribution of crustal material to these calc-alkaline magmas in an early stage of evolution.

K − Ar ages and Sr data of the lamprophyres studied agree with results from Tertiary plutonites in the same geotectonic position. This phase of intense magmatic activity is linked with the continent-continent collision after the second subduction event in the Eastern Alps as proposed by various authors.

Finally, K − Ar data obtained on whole rock samples in three rocks are not sufficient to evaluate an intrusion age. Likewise great care has to be taken in interpreting Sr isotopic ratios of whole rock samples from hypabyssal rocks regarding the nature of the magmas parental source. Our results clearly show that dyke rocks to not represent "closed" Sr systems.

Acknowledgements. I would like to thank Prof. V. Dietrich, Prof. W. Frank (Univ. Wien), F. Oberli and G. Ryder (LPI Houston) for helpful discussions and critical comments of this work. Prof. P. Signer and Prof. H.R. Steiger are gratefully acknowledged for their careful reading of an early draft of the manuscript. I would like to express gratitude to Prof. H.J. Lippolt (Univ. Heidelberg) for his kind permission to let me use the gas mass spectrometer in his labratory. I am grateful to H. Baur for his help with gas mass spectrometer and computer facilities, to P. Bucher for mineral seperation and to M. Lindström for correcting the English. This work has been supported by ETH-Zürich grant 0.330.079.31/0 and by grant 2.480/0.79 from the Swiss National Science Foundation.

References

Alker A, Heritsch H, Paulitsch P, Zednicek W (1952) Malchite aus dem Gailtal. Österr Akad Wiss Sitzungsber Math-Nat Kl Abt I 161:775–783

Bajo S, Wyttenbach (1980) Extraction liquide-liquide des terres rares et application a leur dosage dans les silicates par activation neutronique. E.I.R. Tech Mitt (Internal rep) TM-44-80-2

Baur H (1980) Numerische Simulation and praktische Erprobung einer rotationssymetrischen Ionenquelle für Gasmassenspektrometer. PhD thesis ETH-Zürich Nr. 6596, 94 p

Beck H (1936) Aufnahmsbericht über Blatt Mölltal. Verh Geol B A Wien 1936:43–45

Bellieni G (1980) The Cima di Vila (Zinsnock) massiv: geochemical features and comparisons with the Vedrette di Ries (Rieserferner) pluton (Eastern Alps – Italy). N Jahrb Mineral Abh 138:244–258

Bellieni G, Peccerillo A, Poli G (1981) The Vedrette di Ries (Rieserferner) plutonic complex: petrological and geochemical data bearing on its genesis. Contrib Mineral Petrol 78:145–156

Borsi S, Callegari E, Del Moro A, Ferrara G, Fratta M, Giuliani O, Macera P, Pardini G, Pescia A, Tonarini S, Villa I (1977) Geochronological investigations on the Adamello – Presanella massif. Abstr ECOG V Pisa

Borsi S, Del Moro A, Sassi FP, Zirpoli G (1978a) On the age of the periadriatic Rensen massif (Eastern Alps). N Jahrb Palaeont Monatsh 1978:267–272

Borsi S, Del Moro A, Sassi FP, Zirpoli G (1978b) On the age of the Vendrette di Ries (Rieserferner) massif and its geodynamic significance. Geol Rundsch 68:41–60

Briqueu L, Lancelot JR (1979) Rb–Sr systematics and crustal contamination models for calc-alkaline igneous rocks. EPSL 43:385–396

Canaval R (1895) Die Erzvorkommen im Plattach und auf der Assam-Alm bei Greifenburg in Kärnten und die sie begleitenden Porphyrgesteine. Jahrb Geol R A Wien 45:13–124

Cliff RA, Norris RJ, Oxburgh ER, Wright RC (1971) Structural, metamorphic and geochronological studies in the Reisseck and southern Ankogel groups, the Eastern Alps. Jahrb Geol B A Wien 114:121–272

Cortecci G, Del Moro A, Leone G, Pardini GC (1979) Correlation between strontium and oxygen isotopic compositions of rocks from the Adamello massif (northern Italy). Contrib Mineral Petrol 68:421–427

Dal Piaz GV (1974) Le metamorphisme de haute pression et basse temperature dans l'evolution structurale du bassin ophiolitique alpino-apenninique. Schweiz Mineral Petrogr Mitt 54:399–424

Deutsch A (1980) Alkalibasaltische Ganggesteine aus der westlichen Goldeckgruppe (Kärnten/Österreich). Tschermaks Mineral Petrol Mitt 27:17–34

Deutsch A, Steiger RH (1983) Formation ages vs. cooling ages: K–Ar dating on amphiboles from the Central Alps, Abstr Second EUG Meeting Strassbourg. Terra Cognita 3:180

Dietrich V (1976) Plattentektonik in den Ostalpen. Eine Arbeitshypothese. Geotekt Forsch 50:1–84

Dupuy C, Dostal J, Fratta M (1982) Geochemistry of the Adamello massif (northern Italy). Contrib Mineral Petrol 80:41–48

England PC (1978) Some thermal considerations of the Alpine metamorphism – past, present and future. Tectonophysics 46:21–40

Etique P, Derksen U, Funk H, Horn P, Signer P, Wieler R (1978) Helium, neon, and argon in 61501 agglutinates: implications to gas studies on complex samples. Proc Lunar Planet Sci Conf 9:2233–2267

Exner CH (1961) Der Granodiorit von Wöllatratten (Mölltal) und die hydrothermale Veränderung der diskordanten Ganggesteine der Kreuzeckgruppe. Carinthia II 151:41–50

Exner CH (1976) Die geologische Position der Magmatite des periadratischen Lineamentes. Verh Geol B A Wien 1976:3–64

Frisch W (1978) A plate tectonics model of the Eastern Alps. In: Closs H (ed) Alps, Apennines, Hellenides. E Schweizerbart, Stuttgart, pp 167–172

Frisch W (1981) Plate motions in the alpine region and their correlation to the opening of the Atlantic region. Geol Rundsch 81:402–411

Gatto GO, Gregnanin A, Molin GM, Piccirillo EM, Scolari A (1976) Le manifestationi "andesitiche" polifasiche dell' Alto Adige occidentale nel quadro geodinamico alpino. Studi Trentini di Sci Nat 53:21–47

Gizycki P v, Schmidt K (1978) Zur Genese der Plutone im SW des Tauernfensters (Ostalpen). N Jahrb Geol Palaeont Monatsh 1978:657–673

Gulson BL, Krogh TE (1973) Old lead components in the young Bergell massif, south-east Swiss Alps. Contrib Mineral Petrol 40:239–313

Hammerschmidt K (1981) Isotopengeologische Untersuchungen am Augengneis vom Typ Campo Tures bei Rain in Taufers, Südtirol. Mem Sci Geol Padova XXXIV:273–300

Hansmann W, Oberli F (1983) Typology vs. isotopic age of zircons from the Adamello pluton. Abstr Second EUG Meeting Strassbourg. Terra Cognita 3:138

Hawkesworth CJ (1976) Rb/Sr geochronology in the Eastern Alps. Contrib Mineral Petrol 54:225–244

Hawkesworth CJ, Norry MJ, Roddick JC, Baker PE, Francis PW, Thorpe RS (1979) $^{143}Nd/^{144}Nd$, $^{87}Sr/^{86}Sr$, and incompatible element variations in calc-alkaline andesites and plateau lavas from south America. EPSL 42:45–57

Hawkesworth CJ, Waters DJ, Bickle MJ (1975) Plate tectonics in the Eastern Alps. EPSL 24:405–413

Heritsch H (1971) Neues zur Petrographie zweier Ganggesteine aus Kärnten. Carinthia II Sonderh 28:209–219

Hoernes ST, Friedrichsen H (1974) Oxygen isotope studies on metamorphic rocks of the Western Hohe Tauern (Austria). Schweiz Mineral Petrogr Mitt 54:769–788

Holzer H, Scharbert HG (1958) Über Ganggesteine aus der Kreuzeckgruppe (Kärnten). Verh Geol B A Wien 1958:165–172

Horn P, Lippolt HJ, Todt W (1972) Kalium – Argon-Altersbestimmungen an tertiären Vulkaniten des Oberrheingrabens I. Gesamtgesteinsalter. Eclogae Geol Helv 65:131–156

Irvine TN, Baragar WRA (1971) A guide to the chemical classification of the common volcanic rocks. Can J Earth Sci 8:523–548

Kagami H, Ulmer P, Hansmann W, Oberli F, Dietrich V, Steiger RH (1983) Nd–Sr isotopic characteristics of the southern Adamello intrusives: implications for crustal versus mantle origin. Ann meeting Soc Geol Ital e Soc Ital Mineral Petrol Padova 1983 (Abstr)

Laubscher HP (1983) The tectonic situation of the late Alpine "periadriatic" intrusions. Ann meeting Soc Geol Ital e Soc Ital Mineral Petrol Padova 1983 (Abstr)

Masuda A, Nakamura N, Tanaka T (1973) Fine structures of mutually normalized rare-earth patterns of chondrites. Geochim Cosmochim Acta 37:239–248

Menzies M, Murthy VR (1980) Enriched mantle: Nd and Sr isotopes in diopsides from kimberlite nodules. Nature 283:634–636

Nisbet EG, Dietrich V, Esenwein A (1979) Routine trace element determination in silicate minerals and rocks by X-ray fluorescence. Fortschr Mineral 57:264–279

Oxburgh ER, Lambert RSTJ, Baadsgaard H, Simons JG (1966) Potassium argon studies across the south-east margin of the Tauern Window, the Eastern Alps. Verh Geol B A Wien 1966:17–33

Oxburgh ER, Turcotte DL (1974) Thermal gradients and regional metamorphism in overthrust terrains with special reference to the Eastern Alps. Schweiz Mineral Petrogr Mitt 54:641–662

Pearce JA (1982) Trace element characteristics of lavas from destructive plate boundaries. In: Thorpe RS (ed) Andesites. John Wiley and Sons, pp 525–548

Peccerillo A, Taylor SR (1976) Geochemistry of Eocene calc-alkaline volcanic rocks from the Kastamonou area, Northern Turkey. Contrib Mineral Petrol 58:63–81

Schiffman P, Liou JG (1980) Synthesis and stability relations of Mg–Al pumpellyite, $Ca_4Al_5MgSi_6O_{21}(OH)_7$. J Petrol 21:441–474

Signer P, Baur H, Derksen U, Etique PH, Funk H, Horn P, Wieler R (1977) Helium, neon, and argon records of lunar soil evolution. Proc Lunar Sci Conf 8:3657–3684

Sigvaldason GE (1962) Epidote and related minerals in two deep geothermal drill holes, Reykjavik and Hveragerdi, Iceland. USGS Prof Paper 450E:E77–79

Steiger RH, Jäger E (1977) Subcommission on geochronology: convention on the use of decay constants in geo- and cosmochronology. EPSL 36:359–362

Steiger RH, Hansen BT, Schuler CH, Bär MT, Henriksen N (1979) Polyorogenic nature of the southern Caledonian fold belt in East Greenland: an isotopic age study. J Geol 87:475–495

Takahashi E, Kushiro I, Tasumi Y (1981) Melting of a peridotite and its bearing on island arc magmas. Abstract 1981 IAVCEI symposium on arc volcanism

Teller F (1889) Jahresbericht 1888. Verh Geol R A Wien 1889:5

Thorpe RS, Francis PW (1979) Variation in andean andesite compositions and their petrogenetic significance. Tectonophysics 57:53–70

Trommsdorff V (1962) Über Lamprophyre aus den nördlichen Kalkalpen (Ehrwaldit). Tschermaks Mineral Petrogr Mitt 8:281–325

Wyllie PJ (1981) Plate tectonics and magma genesis. Geol Rundsch 70:128–153

York D (1969) Least squares fitting of a straight line with correlated errors. EPSL 5:320–324

Received March 22, 1983; Accepted September 5, 1983